Dural sinus thrombosis: verification with spin-echo techniques.

G Sze, B Simmons, G Krol, R Walker, R D Zimmerman and M D Deck

AJNR Am J Neuroradiol 1988, 9 (4) 679-686
http://www.ajnr.org/content/9/4/679

Dural Sinus Thrombosis: Verification with Spin-Echo Techniques

Gordon Sze[1]
Byron Simmons[1]
George Krol[1]
Russell Walker[2]
Robert D. Zimmerman[1]
Michael D. F. Deck[1]

Although MR imaging is being used increasingly to detect dural sinus thrombosis, accurate evaluation of images has often been hindered by the presence of artifacts, especially flow-related enhancement, that may simulate intraluminal clot. We tried an approach with spin-echo techniques to eliminate flow-induced artifacts and, thus, facilitate the diagnosis of dural sinus thrombosis. In this investigation, a nonselective single-section spin-echo verification method was used as a prototype of this approach. Both patients and an experimental flow phantom were used to test the validity of this concept. Clinically, thrombosis was seen to persist as isointense or highly intense signal in the vascular lumina with the specialized sequence, while flow-related artifacts were replaced by hypointense signal, but *not* by signal void. These same changes were examined both quantitatively and qualitatively in the flow phantom by using varying velocities of flow.

Although our clinical investigation concerns suspected dural sinus thrombosis, the principles of these specialized spin-echo techniques can be applied successfully throughout the head to eliminate certain flow-related artifacts.

MR imaging is uniquely sensitive both to the evolution of hemorrhage [1] and to blood flow [2–9]. These phenomena follow orderly patterns and rules that lead to generally predictable appearances. Blood clots initially produce hypointense signal but later become markedly hyperintense as the well-known degradation of deoxyhemoglobin to methemoglobin takes place.

Similarly, flowing blood can produce many different appearances, depending on a multitude of interrelated factors [2–9]. Patient factors include the velocity and pulsatile nature of the flow, the orientation of the flow with respect to the gradients, and the fluid dynamics of the flow. Operator-controlled variables are also highly important, especially in terms of the selection of pulse sequences and the positioning and acquisition of sections.

Because of its sensitivity to both blood flow and thrombus formation, MR is used increasingly in place of CT and/or angiography for the evaluation of suspected dural sinus thrombosis [10–15]. Additional methods have been proposed to quantitate flow [16–19]. However, numerous artifacts can result from blood flow. In addition, if thrombus is present, its signal can vary markedly as it evolves [11, 14, 15, 20]. Both phenomena can produce similar MR appearances. Therefore, careful interpretation of images is essential before committing patients to courses of anticoagulation. Although many instances may be obvious on routine spin-echo sequences [11, 15], in certain cases, especially those involving short segments of clot, partial thrombosis, or comparatively small vessels, specialized acquisitions may be necessary.

We have successfully used an alternative approach involving a nonselective 180° refocusing pulse single-section spin-echo method to discriminate between true vascular thrombosis and flow-related artifacts. This method, previously used to image venous flow [19], serves as a prototype of techniques that eliminate flow-related enhancement and thus facilitate detection of intraluminal clot. Both clinical

Received October 10, 1987; accepted after revision February 10, 1988.

[1] Department of Radiology, Memorial Sloan-Kettering Cancer Center and Cornell University Medical College, 1275 York Ave., New York, NY 10021. Address reprint requests to G. Sze, Department of Medical Imaging.

[2] Department of Neurology, Memorial Sloan-Kettering Cancer Center, New York, NY 10021.

AJNR 9:679–686, July/August 1988
0195–6108/88/0904–0679

and experimental techniques were used to test the validity of our approach. Clinically, patients with suspected sinus thrombosis were examined. Experimental verification was obtained through the construction of a flow phantom.

Subjects, Materials, and Methods

Superior Sagittal Sinus Thrombosis

Five patients with suspected superior sagittal sinus thrombosis were imaged on a superconductive magnet operating at 1.5 T with a 25-cm-diameter head coil. There were two male and three female patients, ranging in age from 2–42 years old. Two patients had leukemia and were being treated with L-asparaginase, a chemotherapeutic agent known to cause vascular thrombosis as a side effect. Two patients with systemic tumors had metastases to the skull in the region of the superior sagittal sinus. One patient had marked leptomeningeal deposits of tumor from spread of medulloblastoma.

Initially, T1-weighted sagittal and coronal sequences, 600/20/2 (TR/TE/excitations), and spin-density and T2-weighted axial sequences, 2000/35, 70, were obtained in all cases. In addition, three of the five patients had spin-density and T2-weighted coronal scans. One patient had T1-weighted axial scans. The matrix was 256 × 256, except in one patient in whom long TR sequences were performed with a 256 × 128 matrix owing to the patient's condition. In all T1-weighted sequences, 5-mm sections with an interslice gap of 1 mm were used; in all T2-weighted sequences, 5-mm sections with an interslice gap of 2.5 mm were obtained. In all five of our cases, definitive evaluation of possible dural sinus thrombosis was difficult on the basis of the routine spin-echo sequences. Therefore, all patients had gradient-echo acquisitions (21/12, 30° flip angle) as well. Very short TRs were used to maximize signal from flow. Five-mm sections with an interslice gap of 1 mm were used. The matrix was 256 × 128.

After this examination, the single coronal T1-weighted spin-echo section was chosen that demonstrated findings most consistent with clot. After visualization of suspected clot on standard multislice acquisitions, this single slice was excited by itself by using a selective 90° pulse followed by a nonselective 180° refocusing pulse. Standard spin-echo pulse sequences use a selective 90° pulse followed by selective 180° refocusing pulses, whether single-slice or multislice acquisitions are obtained. With the nonselective pulse, flow-related enhancement is eliminated. If the suspected thrombus proves to be an artifact, it will disappear in the single slice. However, if the thrombus is real, its appearance will remain unchanged. All other imaging parameters were the same as in the multislice coronal T1-weighted sequences.

In all five cases, further evaluation was obtained with traditional methods. This documentation included CT scans on a fourth-generation scanner with contiguous 1-cm axial sections after standard administration of iodinated contrast material. Three of the five patients had coronal scans as well. Four of the five patients also had confirmatory angiograms.

Flow Phantom

For experimental verification, a flow phantom was constructed. A flow pump* providing essentially stable flow with a minimal pulsatile component was used to simulate the venous system. Visually, no perceptible pulsatile component was seen. Rubber tubing with a 3.3-mm internal diameter was used to form a single U-shaped flow channel. The total length of tubing was about 9 m. The portion of the tubing to be imaged was placed with the inflow and outflow arms parallel to the magnetic field and perpendicular to the axial plane. Full magnetization of the fluid was accomplished by coiling the remainder of the inflow portion of the tubing within the bore of the magnet. Even at the maximum velocities, the fluid was subjected to the field for a period of at least 5 × T1. Calibration of flow was performed by measuring the volume with a graduated cylinder for a given interval of time. Seven flow velocities were used and were calculated to be 0, 2.4, 3.4, 6.1, 11.6, 24.2, and 30.6 cm/sec.

The portion of the tubing to be imaged was submerged in a 28 × 36 cm rectangular container filled to a depth of 13 cm. This basin served to hold the stationary background liquid. Both the flowing liquid and the background liquid consisted of water to which copper sulfate was added. The approximate T1 relaxation time of the fluid was 433 msec. The basin was placed in a 25-cm-diameter head coil in the center of the bore of the same 1.5-T imager used in the clinical cases. Scans were obtained perpendicular to the direction of flow. Both short (500 msec) and long (2000 msec) TR multislice spin-echo sequences were performed at all seven velocities of flow. A single echo (20 msec) was used in the T1-weighted sequences; dual echoes (35 and 70 msec) were used in the spin-density and T2-weighted acquisitions. The sections were 1 cm thick and were separated by an interslice gap of 1 cm. The matrix was 256 × 128. After this, the nonselective technique was used in sections displaying increased signal within the tubing. The results on the flow phantom were compared with the clinical cases. Intensity measurements for the selective and nonselective T1-weighted sequences on the flow phantom were calculated by defining a region of interest with the operator-controlled cursor. This region of interest was not changed when different velocities of flow were compared. The velocity of flow was plotted against the ratio of the intensity under conditions of flow to the intensity of stationary fluid.

* Laboratory Supplies Co., Inc., Hicksville, NY.

Results

Superior Sagittal Sinus Thrombosis

On CT and/or angiography, three of the five patients were shown to have superior sagittal sinus thrombosis (Table 1). CT scans in two of the five patients showed the "empty delta" sign. These patients were considered positive. In one of the five patients, who had a clot in the anterior portion of the sinus, CT scans were not conclusive, even when coronal scans were obtained with careful windowing on the monitor (Fig. 1A). Angiography in this patient showed probable truncation of the anterior portion of the sinus and was considered positive. Of the other three patients who underwent angiography, findings were negative in two and positive in one. In the positive case the patency of the superior sagittal sinus and left transverse sinus could not be demonstrated throughout most of their course. Rather, extensive serpiginous collateral vessels were noted.

On the T1-weighted coronal MR sequences, all five patients showed foci of high signal in the expected course of the superior sagittal sinus (Figs. 1 and 2). In all patients, the findings were localized, often to only the anterior or middle portion of the sinus. On the T1-weighted sagittal MR sequences, regions of thrombosis were suspected in four of the five studies. Instead of signal void seen throughout the course of the sinus, some signal appeared to be present filling certain segments of the sinus. This signal varied from isointense to hyperintense relative to surrounding brain parenchyma. However, in no cases did signal fill the entire course of the sinus; rather, signal void was noted in considerable lengths of the

TABLE 1: Imaging Findings in Patients with Suspected Dural Sinus Thrombosis

Case No.	Age	Gender	Diagnosis	MR Findings					Enhanced CT	Angiography
				T1 Coronal	T1 Sagittal	T2 Coronal or Axial	Gradient Echo	Nonselective		
1	2	M	Leukemia, on L-asparaginase	High signal in SSS on five of nine slices	?Short segments of mild hyperintensity in SSS	Hyperintense signal in SSS	Low signal in SSS with some foci of high signal, suggesting thrombus	High signal in SSS	Empty delta sign	NA
2	37	F	Breast carcinoma metastatic to skull	High signal in SSS on four of nine slices	?Short segments of isointensity in SSS	Isointense signal in SSS	High signal in SSS suggesting flow	Mildly hypointense signal in SSS	Negative in axial and coronal for delta sign	Negative, slow flow in SSS
3	17	F	Leukemia, on L-asparaginase	High signal in SSS on three of nine slices	Short segments of high signal in SSS	?Hyperintense signal in SSS, more obvious on first echo	Equivocal	High signal in SSS	Negative in axial and coronal for delta sign	Positive
4	4	M	Medulloblastoma with subarachnoid spread	High signal in SSS on six of nine slices; patent collateral seen	Isointense signal in most of SSS	Hyperintense signal in SSS; hypointense vascular signal adjacent to it	Low signal in SSS suggesting thrombosis with small focus of high signal laterally	High signal in SSS; patent adjacent collateral	Empty delta sign	Positive
5	42	F	Breast carcinoma metastatic to skull	High signal in SSS on four of nine slices	Short segments of isointensity in SSS	Isointense signal in SSS	High signal in SSS suggesting flow	Mildly hypointense in SSS	Negative in axial for delta sign	Negative

Note.—SSS = superior sagittal sinus; NA = not applicable.

sinus. In one case, no definite clot was detected. Signal void appeared to be present throughout the course of the sinus as it was followed on several adjacent sections. T2-weighted axial or coronal sequences showed some signal in the sinus in all five patients. Gradient-echo acquisitions were positive in two of the five patients, negative in two, and equivocal in one.

On the nonselective examinations, unequivocal high signal was seen in the superior sagittal sinus in three patients (Fig. 1). This signal appeared identical in size and intensity to the findings on the multislice acquisitions (Fig. 2). These patients were considered positive by the criteria of this study. In two of the five patients, only mildly hypointense signal appeared in the sinus, in contrast to the high signal seen on the multislice acquisitions. These patients were considered negative. The results of the nonselective technique correlated with those of CT and/or angiography.

Not surprisingly, all patients showed high signal in the course of the superior sagittal sinus on T1-weighted coronal images in several sections, yet only three were positive for thrombus. Evaluation of the course of the sinus on sagittal scans did not show large segments of signal in any of the patients included in this study, although we have certainly seen other patients in whom thrombus was easily imaged in this projection. Since no question arose in these other cases, the nonselective technique was not used and these patients were not included in the present study. Signal was also present in the sinus on T2-weighted scans in all cases; yet, again, in two of these patency was proved by angiography.

The specialized sequences were very accurate in our evaluation. Gradient-echo acquisitions easily assessed cases of normal flow. In one patient who later proved to have thrombosis, findings were equivocal. In another patient, probable thrombosis was seen, but the presence of some small foci of

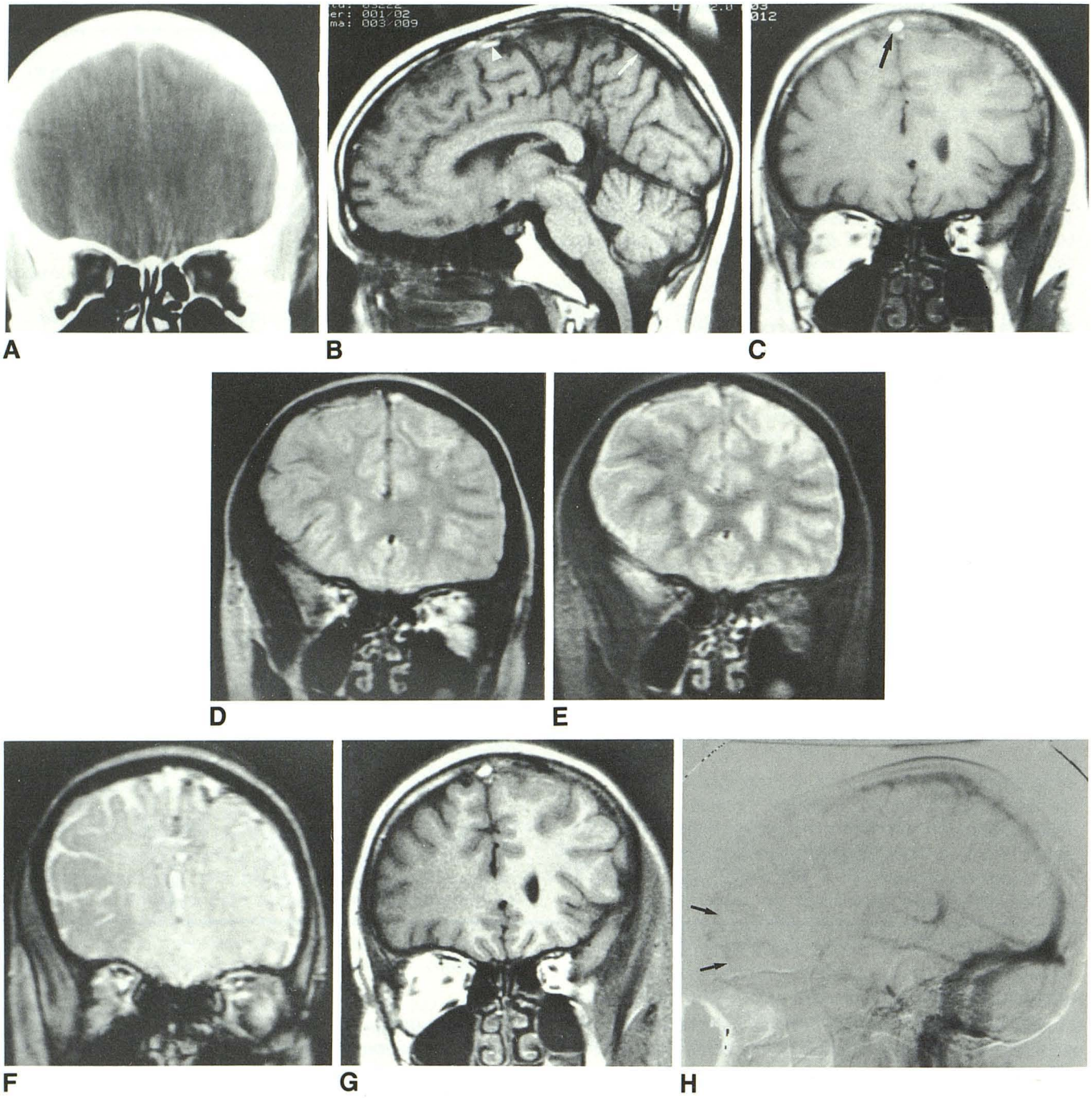

Fig. 1.—Case 3: 17-year-old girl with leukemia, on L-asparaginase, presenting with multiple seizures.

A, Coronal enhanced CT section is equivocal with respect to definitive diagnosis of superior sagittal sinus thrombosis.

B, T1-weighted sagittal image, 600/20, shows clearly patent superior sagittal sinus posteriorly (*arrow*). However, short segments of signal appear to be present anteriorly (*arrowhead*).

C, T1-weighted coronal image, 600/20, shows high signal in course of sinus (*arrow*), consistent with both thrombosis and entry phenomenon.

D and *E*, Long TR coronal images, 2000/35 (*D*) and 2000/70 (*E*). Focus of high signal on first echo is not easily seen on second echo.

F, Gradient-echo image, 21/12 (30° flip angle), does not disclose unequivocal lack of flow in superior sagittal sinus. In fact, venous thrombosis was not easy to diagnose on this sequence. Sequelae of thrombosis include small, mildly hemorrhagic venous infarct on left.

G, Nonselective single-slice T1-weighted image, 600/20, reveals persistent high intensity in dural sinus. Appearance is virtually identical to section from multislice acquisition (*B*) and suggests that thrombus, not artifact, has produced this signal.

H, Digital IV angiogram does not show patent superior sagittal sinus posterior to coronal suture. While hypoplasia of anterior portion of superior sagittal sinus can occur, it is usually anterior to coronal suture. In addition, existence of sinus anteriorly in this case was clear from MR scans. Some early collaterals may be present in frontal region (*arrows*).

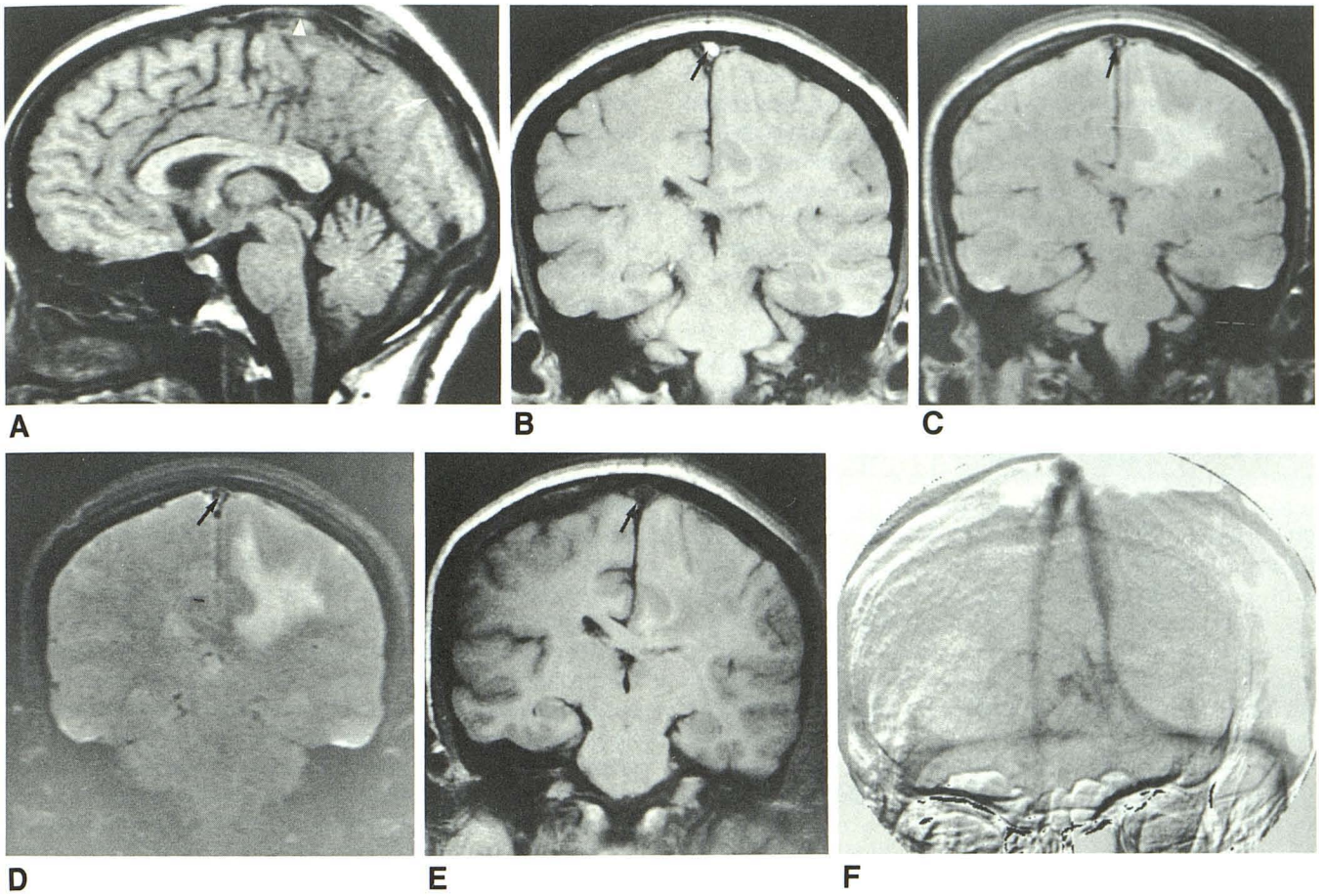

Fig. 2.—Case 2: 37-year-old woman with breast carcinoma and large skull metastasis, presenting with headache.

***A*, T1-weighted sagittal image, 600/20, shows patent superior sagittal sinus posteriorly (*arrow*), with possible signal in its mid course (*arrowhead*), as in Fig. 1A.**

***B*, T1-weighted coronal scan, 600/20, shows high intensity in course of sinuses (*arrow*). This signal was visible on five of 12 adjacent sections anteriorly.**

***C* and *D*, Long TR coronal images, 2000/35 (*C*) and 2000/70 (*D*), disclose apparent signal in course of sinus (*arrows*). High intensity in brain parenchyma on left is due to edema created by protruding skull metastasis posteriorly.**

***E*, Nonselective single-slice T1-weighted coronal scan, 600/20, shows loss of high signal, which was noted in multislice acquisition in superior sagittal sinus (*arrow*). This change in appearance confirms presence of flow-related artifact in original sequence. Note that hypointense signal, rather than signal void, is now present in sinus. This signal should not be mistaken for thrombus.**

***F*, Confirmatory digital IV angiogram. Mild delay in flow is seen in superior sagittal sinus anterior to large skull metastasis, but no thrombosis is present.**

high signal was noted. The nonselective method was accurate in all five patients. It was able to depict both clot and the presence of collaterals.

Flow Phantom

Results with the flow phantom provided experimental correlation with the clinical findings (Fig. 3). Slowly moving fluid at speeds of up to about 6 cm/sec produced high signal on short TR sequences due to flow-related enhancement. However, with the nonselective refocusing pulse, the high signal was replaced by signal that was hypointense relative to that seen in nonmoving fluid. At speeds of about 6–11 cm/sec, increasing peripheral signal void was noted on both the selective and nonselective acquisitions. These results were also demonstrated graphically (Fig. 4). On the long TR sequences, signal on the first-echo image was noted within the tubing at speeds of up to 11.6 cm/sec. No even-echo rephasing was seen in our flow phantom. Signal was lost after the second 180° pulse between 6.1 and 11.6 cm/sec, earlier than after the first 180° pulse as velocities of flow were increased.

Discussion

Traditionally, both angiography and CT have been used for the diagnosis of dural sinus thrombosis. Although accurate, angiography is obviously invasive. In specific situations, for example, assessment of possible superior sagittal sinus thrombosis, CT has been used as a less invasive alternative [21, 22]. CT has a documented sensitivity of only 75%, however, and careful examination at intermediate windows may be needed for detection. In addition, superior sagittal sinus thrombosis localized to the anterior or mid portions of the sinus necessitates coronal CT sections, which are not

routine and may not be possible in many patients because of difficulty in positioning. Both angiography and CT also require substantial amounts of iodinated contrast material.

MR is very sensitive to the orderly evolution of hemoglobin breakdown that intraluminal thrombosis undergoes [1, 15]. In addition, MR also can accurately depict regions of flow [2–9]. Thus, it is being used increasingly in the assessment of possible vascular thrombosis [10–13, 16]. However, for a number of well-described reasons, flowing blood, especially when slow, can often cause artifactually high signal [2–9]. Flowing blood usually leads to signal void, explained by either flow of spins out of the imaged volume between the 90° detection pulse and the 180° refocusing pulse [2] or by spin-phase changes created by the movement of spins in a gradient field [3, 12]. However, visualization of signal within vascular lumina is, of course, extremely common and can occur by several mechanisms. First, slowly moving, fully magnetized protons can enter the imaged volume and replace partially saturated spins. When this process occurs in a period of time less than or equal to the T1 relaxation time of surrounding tissues, the signal of the vessel lumen will increase on the initial slices of a multislice acquisition [2, 4, 8]. This effect is more prominent on short TR sequences. Second, slowly moving protons undergo more complete rephasing of spins after even-numbered 180° refocusing pulses, producing increased signal on even-numbered echoes [2, 6, 8, 9]. A similar mechanism produces signal on all echoes when gradient moment nulling techniques are implemented. Third, protons in flowing blood can be present within the imaged volume for the first 180° pulse but then flow out of the slice by the time of the second 180° pulse or subsequent pulses [6, 12]. This phenomenon produces intravascular signal on early echoes only. At an extreme, stagnant blood can be seen as high signal on all echoes of a long TR sequence [23]. Finally pseudogating of pulsatile flow can also produce signal within vessel lumina, dependent on the chance synchronization of heart rate and TR [2]. Because of these mechanisms, flowing blood can create signal that can appear on both short and long TR sequences and on both first or second echoes. This signal can be mistaken for thrombus formation.

One additional point needs emphasis. It has been stated that flow-related enhancement can be distinguished from thrombus because it occurs on entry slices and diminishes progressively. However, Valk et al. [4] have pointed out that in multislice imaging, enhancement in deeper sections depends on the exposure of spins to 90° pulses in preceding sections. Enhancement can follow a bimodal pattern in consecutive sections with two peaks, one due to "low-velocity enhancement" and one due to "high-velocity enhancement."

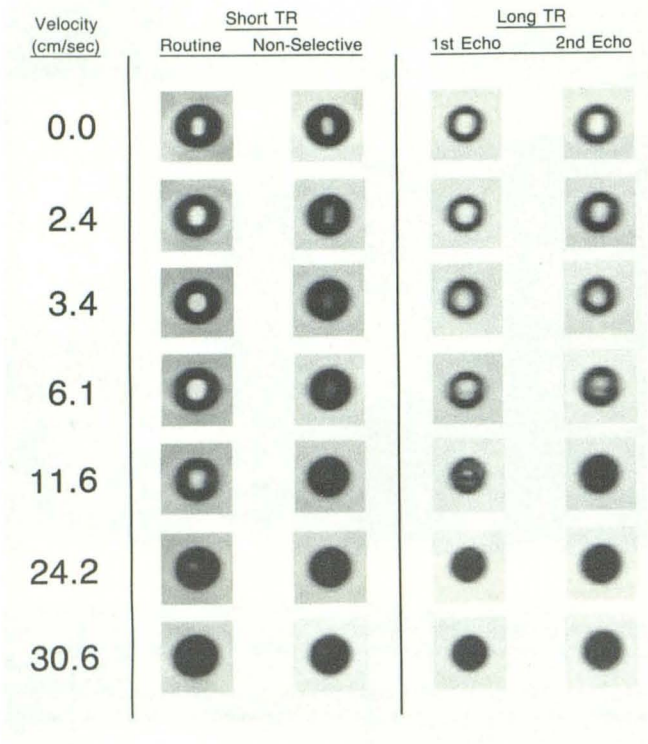

Fig. 3.—Flow phantom experiment. Under *Short TR* are sections from short TR multislice acquisition (*left side*) and results of nonselective single slice technique (*right side*). Note that flow-related enhancement is eliminated. Under *Long TR* are sections from long TR multislice sequence.

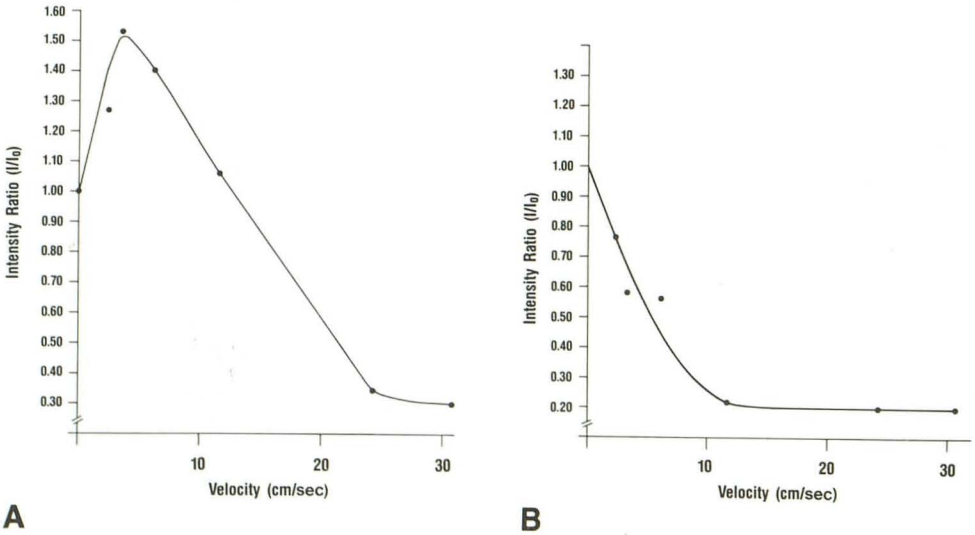

Fig. 4.—Graphs of velocity of flow plotted against I/I_0 in phantom, where I = intensity under conditions of flow and I_0 = intensity of static fluid.

***A*, Multislice selective T1-weighted acquisition, 600/20, shows flow-related enhancement at low velocities with later evolution of signal void at higher velocities.**

***B*, Nonselective single-slice T1-weighted acquisition, 600/20, shows decrease in signal intensity with low velocities, followed again by signal void at higher velocities. In reality, graph probably has two plateaus. The first, at low velocity (less than 10 cm/sec), represents loss of flow-related enhancement. The second, at high velocity (greater than 10 cm/sec), results from dephasing of moving spins and/or from flow of spins out of imaged volume between excitation and refocusing pulses.**

Because of this, it can be difficult to differentiate flow-related enhancement from thrombosis on the basis of the MR signal patterns since the artifact may appear more prominent on deeper slices than on more superficial slices. Added to these effects is the fact that the acquisition of sections in most machines does not occur sequentially, thereby diminishing cross excitation.

Different MR methods have been suggested to eliminate the possibility of flow-related artifacts [11–16]. First and simplest, the suspected thrombosis should be seen on at least two different sequences, which may vary in plane of section or in TR. In superior sagittal sinus thrombosis, it may be difficult to find two projections that both demonstrate the abnormality. Coronal or axial scans are obviously situated perpendicular to much of the course of the superior sagittal sinus and are ideal to assess the possibility of clot in this structure. However, they are also susceptible to flow-related enhancement. If clot in the sinus is also seen on the sagittal scans, these findings together likely constitute sufficient proof of thrombosis. Yet sagittal scans sometimes do not image enough of the sinus in a single section to enable confident diagnosis of thrombosis. This difficulty is particularly significant when thrombosis is limited to small segments of the sinus.

Visualization of suspected clot on two separate sequences with widely varying TRs can be unreliable. The possibility of flow-related enhancement as a cause of high signal within the lumen of the vessel on T1-weighted images is well known. However, signal can also be seen in vasculature on long TR sequences after both odd- and even-echo delays, as mentioned above [2, 6, 8, 9, 12]. Therefore, the appearance of signal within a vessel on both short and long TR sequences is not necessarily diagnostic of thrombosis. In fact, flow-related artifacts frequently produce these findings. We have seen high signal appear in lumina of patent superior sagittal sinuses on both T1- and T2-weighted images as the result of comparatively stagnant nonthrombosed blood (Fig. 2). Conversely, even if no identifiable signal arises from vessels on T2-weighted sequences, thrombus cannot be excluded since intraluminal clot evolves in stages that parallel those of extravascular blood [15]. Until breakdown of deoxyhemoglobin to methemoglobin occurs, usually on the order of several days, thrombus will be hypointense on T2-weighted images [1]. Therefore, lack of visualization of intraluminal intensity on long TR sequences does not preclude the possibility of thrombus.

Other MR imaging methods that have been suggested to differentiate flow-related artifacts from thrombus include phase-imaging techniques [12, 13, 16, 18]. The occurrence of a parallel collateral supply, seen in one of our cases, might prompt a falsely negative conclusion. The presence of partial thrombosis also might not be depicted accurately.

Gradient-echo acquisitions are also extremely sensitive to flow and often sufficient. However, in their current state, they may not provide sufficient resolution, especially in cases of partial thrombosis, substantial collateral supply, or small-vessel involvement. In one of our angiographically proved cases, gradient-echo images appeared to show some flow on the thrombosed section (Fig. 1). No substantial collaterals were seen on the digital IV subtraction study.

Spin-echo techniques that eliminate flow-related enhancement have several advantages over the methods listed above. The nonselective single-section method described here serves as a prototype for this alternative approach. Standard spin-echo imaging uses a 90° pulse followed by 180° pulses, all selective in the slice-selection gradient direction. In this flow imaging scheme, the 90° pulse is selective in the slice-selection direction, but the 180° pulse is, in effect, nonselective. Although this refocusing pulse is termed "nonselective," in reality it is nonselective in the y and z axes but selective in the x axis to the extent of the field of view chosen. Since the field of view is large, for practical purposes, the 180° refocusing pulse is nonselective. Partially saturated spins that leave the imaged volume are replaced by partially saturated spins from outside the slice. Therefore, augmentation of signal from time-of-flight effects cannot occur (Fig. 3). Alternative methods of suppressing flow-related enhancement also have been described. Wehrli et al. [3] discussed a method that uses a preliminary nonselective 90° saturation pulse followed by selective 90° detection and 180° refocusing pulses. They also noted the similarity of this nonselective tagging pulse to a 180° nonselective refocusing pulse.

Because all of these techniques eliminate flow-related enhancement, they can be used successfully to differentiate thrombosis from flow artifacts. True thrombosis should appear unchanged in the specialized sequence; flow-related artifacts will disappear. In addition, because a spin-echo technique, rather than a gradient-echo acquisition or phase-shift method, is used, images can be obtained that are as detailed and concise as in the multislice sequences. Precise anatomic comparisons are possible. Partial thrombosis and collaterals can be demonstrated accurately. Finally, elimination of intravascular artifactual signal also results in suppression of much of the phase-shift "ghosting" that occurs along the phase-encoding axis. One caveat must be mentioned: Very acute and chronic clot may be mildly hypointense rather than hyperintense on T1-weighted images. This appearance is particularly typical of tumor thrombus and of long-standing vascular thrombosis. In these cases, confusion with flow-related enhancement is less likely, and the nonselective spin-echo method does not have a role.

The signal in both the clinical cases and experimental model after the suppression of flow-related enhancement was more hypointense than would be expected from static fluid, although signal void did not result. Most likely, this decrease in signal resulted from flow of partially saturated spins out of the imaged section and replacement by even more saturated spins [8] or from gradient-induced phase effects arising from spins flowing in a velocity distribution across each pixel [3]. This latter phenomenon also was responsible for the loss of signal at the periphery of the moving liquid in all of the flow phantom sequences as velocity increased [3] (see Appendix).

It is important to note that suppression of flow-related enhancement did *not* create signal void. Therefore, when using the nonselective method to eliminate this artifact, some signal was still seen in the vessel lumen. Clinically, this hypointense signal will be present with any technique that eliminates flow-related enhancement and should not be mistaken for thrombosis (Fig. 2E).

Exact correlation between the appearance of liquid flowing at specific velocities in the flow phantom and of flowing blood in arteries and veins is difficult for several reasons. These reasons include differences between the flowing liquid and blood with respect to their relaxation times, viscosity, and flow profile. Other variables involve differences in the diameter, shape, and composition of the phantom tubing compared with actual vessels. Finally, the section thicknesses and interslice gaps used in the clinical cases varied from those used in the phantom studies. For example, the optimal speed to achieve maximal flow-related enhancement in the initial slice of an acquisition is dz/TR, where dz is the section thickness. This velocity theoretically would be 0.5 cm/0.6 sec or 0.83 cm/sec for the clinical cases compared with 1 cm/0.5 sec or 2 cm/sec for the phantom studies.

In conclusion, we have applied specialized spin-echo sequences to eliminate certain flow-related artifacts and to study dural sinus thrombosis. Although the technique used here employs a single-slice nonselective 180° refocusing pulse, the approach can also be modified to multislice sequences. Our investigation focused on dural sinus thrombosis; however, the method is applicable to intravascular clot at any site in the head or elsewhere and seems especially useful in thrombosis of fairly small vessels that may not be assessed easily by other methods. We have also used it in the assessment of possible internal jugular vein thrombosis. Alternatively, this technique should be useful to rule out thrombus formation in giant aneurysms. While many cases of thrombosis may be obvious with routine spin-echo imaging, this technique adds another method with which to analyze problems of flow and vascular occlusion.

Appendix

Flow in a small channel, as was used in our experimental model, has a greater tendency to be laminar than flow in larger channels [6]; and in laminar flow, gradient-induced phase shifts in each pixel are largest near the vessel wall itself. In our experimental model, nearly all signal disappeared from the lumen of the tubing by about 10 cm/sec on both the selective and nonselective sequences. These results correlate closely with those of Valk et al. [4]. Again, since the signal loss was initially primarily peripheral, it more likely was caused by dephasing of spins than by high-velocity outflow of signs. The latter would result in central loss of signal in a laminar flow model. Additional proof that dephasing of spins rather than high-velocity signal loss was operative is evident because of the velocity of the fluid at which the hypointensity occurred was not sufficient to produce outflow of spins between the 90° and 180° pulses. When spins flow at a velocity greater than dz/½TE, where dz is the section thickness, then high-velocity signal loss will occur [2]. In our phantom, these calculations would require a velocity of approximately 100 cm/sec for the short TR sequences and of approximately 58.8 cm/sec for the first echo and 19.2 cm/sec for the second echo of the long TR sequences. Clearly, these velocities are considerably faster than most of the velocities involved in our experimental situation.

REFERENCES

1. Gomori JM, Grossman RI, Goldberg HI, Zimmerman RA, Bilaniuk LT. Intracranial hematomas: imaging by high-field MR. *Radiology* **1985**;157:87–93
2. Bradley WG Jr, Waluch V. Blood flow: magnetic resonance imaging. *Radiology* **1985**;154:443–450
3. Wehrli FW, Shimakawa A, MacFall JR, Axel L, Perman W. MR imaging of venous and arterial flow by a selective saturation-recovery spin echo (SSRSE) method. *J Comput Assist Tomogr* **1985**;9(3):537–545
4. Valk PE, Hale JD, Crooks LE, et al. MRI of blood flow: correlation of image appearance with spin-echo phase shift and signal intensity. *AJR* **1986**;146:931–939
5. George CR, Jacobs G, MacIntyre WJ, et al. Magnetic resonance signal intensity patterns obtained from continuous and pulsatile flow models. *Radiology* **1984**;151:421–428
6. Bradley WG Jr, Waluch V, Lai KS, Fernandez EJ, Spalter C. The appearance of rapidly flowing blood on magnetic resonance images. *AJR* **1984**;143:1167–1174
7. Dinsmore RE, Wedeen VJ, Miller SW, et al. MRI of dissection of the aorta: recognition of the intimal tear and differential flow velocities. *AJR* **1986**;146:1286–1288
8. Axel L. Blood flow effects in magnetic resonance imaging. *AJR* **1984**;143:1157–1166
9. von Schulthess GK, Higgins CB. Blood flow imaging with MR: spin-phase phenomena. *Radiology* **1985**;157:687–695
10. Erdman WA, Weinreb JC, Cohen JM, Maximilian Buja L, Chaney C, Peshock RM. Venous thrombosis: clinical and experimental MR imaging. *Radiology* **1986**;161:233–238
11. McMurdo SK Jr, Brant-Zawadzki M, Bradley WG Jr, Chang GY, Berg BO. Dural sinus thrombosis: study using intermediate field strength MR imaging. *Radiology* **1986**;161:83–86
12. White EM, Edelman RR, Wedeen VJ, Brady TJ. Intravascular signal in MR imaging: use of phase display for differentiation of blood-flow signal from intraluminal disease. *Radiology* **1986**;161:245–249
13. Dinsmore RE, Wedeen V, Rosen B, Wismer GL, Miller SW, Brady TJ. Phase-offset technique to distinguish slow blood flow and thrombus on MR images. *AJR* **1987**;148:634–636
14. Glazer HS, Gutierrez FR, Levitt RG, Lee JKT, Murphy WA. The thoracic aorta studied by MR imaging. *Radiology* **1985**;157:149–155
15. Macchi PJ, Grossman RI, Gomori JM, Goldberg HI, Zimmerman RA, Bilaniuk LT. High field MR imaging of cerebral venous thrombosis. *J Comput Assist Tomogr* **1986**;10(1):10–15
16. Moran PR, Moran RA, Karstaedt N. Verification and evaluation of internal flow and motion. *Radiology* **1985**;154:433–441
17. Young IR, Bydder GM, Payne JA. Flow measurement by the development of phase differences during slice formation in MR imaging. *Magn Reson Med* **1986**;3:175–179
18. Bryant DJ, Payne JA, Fermin DN, Longmore DB. Measurement of flow with NMR imaging using a gradient pulse and phase difference technique. *J Comput Assist Tomogr* **1984**;8:588–593
19. Wehrli FW, MacFall JR, Axel L, Shutts D, Glover GH, Herfkins RJ. Approaches to in-plane and out-of-plane flow imaging. *Noninvasive Med Imaging* **1984**;1:127–136
20. Goldberg HI, Grossman RI, Gomori JM, Asbury AK, Bilaniuk LT, Zimmerman RA. Cervical internal carotid artery dissecting hemorrhage: diagnosis using MR. *Radiology* **1986**;158:157–161
21. Goldberg AL, Rosenbaum AE, Wang H, Kim WS, Lewis VL, Hanley DF. Computed tomography of dural sinus thrombosis. *J Comput Assist Tomogr* **1986**;10:16–20
22. Brant-Zawadzki M, Chang GY, McCarty GE. Computed tomography in dural sinus thrombosis. *Arch Neurol* **1982**;39:446–447
23. Olsen W, Kucharczyk W, Brant-Zawadzki M, Norman D, Newton TH. The MR characterization of non-flowing intravascular blood. *Acta Radiol [Suppl]* (Stockh) **1986**;369:63–66